AIMS | African Institute for Mathematical Sciences CAMEROON

Blood Flow in an Inclined Tapered Stenosed Porous Artery under the Influence of Magnetic Field and Heat Transfer

Adeyemi Damilare Adeoye (adeyemi.adeoye@aims-cameroon.org)
African Institute for Mathematical Sciences (AIMS)
Cameroon

Supervised by: Dr. Jos Usman Abubakar
University of Ilorin, Ilorin, Nigeria

18 May 2018
Submitted in Partial Fulfillment of a Structured Masters Degree at AIMS-Cameroon

Abstract

A tapered inclined porous artery with stenosis was considered under the influence of magnetic field and heat transfer. The mathematical formulation for the momentum and energy equations of the blood flow considered to be Newtonian were obtained. The energy equation which was obtained by taking an extra factor of heat source and the nonlinear momentum equation were simplified under the assumption of mild stenosis. These equations were non-dimensionalized and solved using Differential Transform Method (DTM) to obtain expressions for velocity, temperature and volumetric flow rate. The graphs of the expressions were plotted against radius of the artery to simulate the effects of magnetic field, heat transfer and other fluid parameters on the velocity, temperature and the volumetric flow rate of the blood. It was observed that as the magnetic field parameter (M) increases, the velocity, temperature and the volumetric flow rate of the blood increase but wall shear stress decreases at the stenosis throat. It was further observed that the effects of heat transfer and magnetic field resulted into a greater variation in the volumetric flow of an inclined artery in the converging region than in the diverging region.

Declaration

I, the undersigned, hereby declare that the work contained in this essay is my original work, and that any work done by others or by myself previously has been acknowledged and referenced accordingly.

Adeyemi Damilare Adeoye, 18 May 2018.

Contents

1. General Introduction

1.1 Introduction

Blood is a suspension of erythrocytes (red blood cells), leukocytes (white blood cells), and platelets in an aqueous electrolyte solution known as plasma. In normal blood, erythrocytes constitute 45% of the total volume of blood. This volumetric fraction of the erythrocytes defines an important variable called hematocrit.

Stenosis, a constriction in blood vessels, is one of the leading causes of death in many countries of Africa and the world at large. Severe stenosis reduces the blood supply, thereby causing critical flow conditions which results in serious effects called carotid artery blockage, a major contributing factor to strokes [23]. This results from the brain not receiving enough blood as the plague builds up and hardens down the artery. When the brain lacks adequate supply of blood, the cells in it begin to die. This leads to severe disability or death of an individual. Due to these risks, it is important to watch out for the symptoms of a carotid artery blockage, like the Transient Ischemic Attack (TIA) and stroke, so that proper measures can be taken before the condition gets worse.

The study of fluid dynamics has enabled many researchers to examine the mathematical and physical behaviour of blood as it circulates in the blood vessels.

1.2 Aim and Objectives

The aim of this work is to study the influence of external magnetic field and heat transfer on blood flow in an inclined tapered porous artery with stenosis.

The following were the objectives of the study:

- to develop equations of motion for modeling blood flow in a stenotic tapered inclined porous artery under the assumptions made.
- to find a numerical solution to our modeled equations using the Differential Transform Method (DTM).
- to analyze and simulate, using Mathematica generated codes, the effects of the inclination angle, the magnetic field and heat source parameters on blood flow velocity, temperature and volumetric flow rate through graphs.

1.3 Background of Study

In the past decades, many investigators have displayed interest in problems arising from blood flow mechanism and characteristics under different conditions and influence of external factors.

The idea of electromagnetic fields in medical research was first given by Kolin [9] and the possibility that the application of magnetic field to blood would regulate its movement in human system was later

studied by Korchevskii and Marochnik [10]. Abdullah *et al.* [1] and Bose and Banerjee [3] discussed magnetic particle capture for biomagnetic fluid flow in stenosed aortic.

The above mentioned authors observed that the effect of magnetic field is to slow down the speed of blood. But, they did not analyze the magnetic effect on blood flow through an inclined artery. If a magnetic field is applied to an electrically conducting fluid in motion, electric and magnetic fields are induced which interact and a body force known as Lorentz force is produced, and has a propensity to either assist or oppose the fluid motion. Chakraborty *et al.* [4] analyzed the suspension of blood flow through an inclined tube with an axially non-symmetric stenosis.

In the case of stenosis when the cholesterol deposits on the wall of the artery, the artery-clogging blood which clots inside the lumen of the coronary artery is considered as being equivalent to a fictitious porous medium. This case is particularly examined by some researchers. El-Shahed [7] presented a model for pulsatile blood flow through a stenosed porous artery under the effect of periodic body acceleration. Akbarzadeh [2] presented a numerical simulation of the effect of periodic body acceleration and periodic body pressure gradient on magneto-hydrodynamic (MHD) blood flow through porous artery. All of these published works, however, do not include the analysis of blood flow characteristics through an inclined artery with the applied magnetic field, which was presented by Srivastava [23].

Blood viscosity, although constant in real physiological system, it may vary in ratio of hematocrit or depend on temperature and pressure [22]. Massoudi and Christie [12], Pantokratoras [16], Nadeem and Akbar [14] analyzed the influence of heat transfer with temperature dependent viscosity. Petrofsky [18] examined the effect of the moisture content of heat source on the blood flow response of the skin through data. Prakash *et al.* [20] developed a model for bifurcated arteries to analytically study the effects of heat source on magneto-hydrodynamic (MHD) blood flow.

In this work, we present combined effects of the external heat source and magnetic field on an inclined tapered stenosed porous artery, considering variable viscosity of the blood flow. Under well-defined boundary conditions, the resulting non-linear differential equations of the model have been solved numerically using Differential Transform Method (DTM).

2. Concepts, Assumptions and Basic Equations

2.1 Introduction

In this chapter, we will describe the Lagrangian and Eulerian flow concepts and define Newtonian and Non-Newtonian fluids. In our model, blood will be considered an incompressible Newtonian fluid. We will consider temperature and pressure dependent blood viscosity. Our model equations will be derived in this chapter, from the continuity equation, the momentum equations and the energy equation. The resulting equations will be solved numerically in chapter 3 using the Differential Transform Method.

2.2 Description of a Flow

In order to describe a flow, we either use the 'Lagrangian' description or the 'Eulerian' description [5]:

2.2.1 Lagrangian Description of a Flow. Consider a fluid flow where each constituent particle carries its own flow properties such as density ($\rho_p(t)$), velocity ($\vec{v}_p(t)$), pressure ($p_p(t)$), etc. As the particle moves, its properties may change in time. The law of conservation of mass and Newton's law apply to each fluid particle.

This description of fluid flow in which detailed properties of each fluid particle is taken into account is known as the Lagrangian description.

2.2.2 Eulerian Description of a Flow. We can otherwise decide to keep record of how the flow properties change as time changes, at every point in space - That is, the flow properties at a specified location depend on the location and on time. For example, the velocity ($\vec{v}$), density (ρ), pressure (p), etc, of the flow can be described by position and time, and this may allow us to write $\vec{v}(\vec{x},t)$, $p(\vec{x},t)$, $\rho(\vec{x},t)$, etc.

2.2.3 The Material (or Substantial) Derivative. The material derivative denoted by D/Dt, is a Lagrangian concept. It is defined as the rate of change of a flow property associated with a fluid particle 'p' with respect to time.

We can express the material derivative in terms of Eulerian quantities, say $f(\vec{x},t)$, so that the conservation laws can be applied in the Eulerian reference frame.

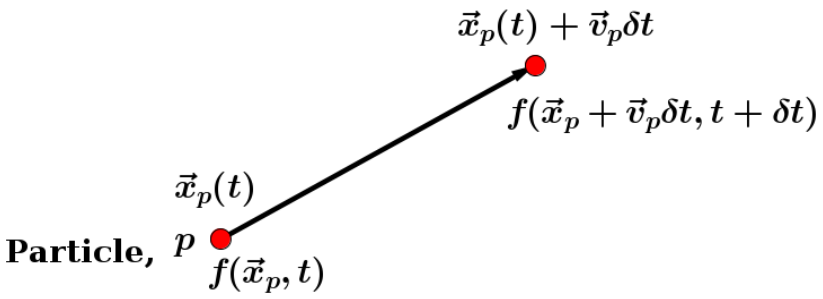

Figure 2.1: Substantial derivative of a property f relative to the motion of a particle p

The rate at which f changes with respect to time relative to a particle 'p' moving with a velocity $\vec{v}_p$ is the substantial derivative of f given by [5]

$$\frac{Df(\vec{x}_p,t)}{Dt} = \lim_{\delta t\to 0} \frac{f(\vec{x}_p+\vec{v}_p\delta t, t+\delta t) - f(\vec{x}_p,t)}{\delta t}. \tag{2.2.1}$$

By Taylor Series expansion about $(\vec{x}_p,t)$ and noting that $\vec{v}_p = \delta\vec{x}/\delta t$, we have

$$f(\vec{x}_p+\vec{v}_p\delta t, t+\delta t) = f(\vec{x},t) + \delta t\frac{\partial f(\vec{x},t)}{\partial t} + \delta\vec{x}\cdot\nabla f(\vec{x},t) + O(\delta^2). \tag{2.2.2}$$

From (2.2.1) and (2.2.2), neglecting $O(\delta^2)$ and higher order terms in (2.2.2), we see that the material derivative of f is given by:

$$\frac{Df}{Dt} = \frac{\partial f}{\partial t} + \vec{v}_p\cdot\nabla f.$$

In general notation, we write [5]

$$\underbrace{\frac{D}{Dt}}_{Lagrangian} = \underbrace{\frac{\partial}{\partial t} + \vec{v}_p\cdot\nabla}_{Eulerian}. \tag{2.2.3}$$

The flow described by (2.2.3) is said to be steady if $\partial/\partial t \equiv 0$. The flow is said to be incompressible if $D/Dt \equiv 0$.

A steady flow is a strictly Eulerian concept while an incompressible flow is a strictly Lagrangian concept [5].

2.3 Viscosity: Newtonian and Non-Newtonian Fluids

Viscosity is defined as the internal stickiness of a fluid [19]. It is a quantity that describes a fluid's resistance to flow. Newton (1642 - 1727) observed that if a substance is heated, it will become less viscous and if cooled, it will become more viscous. He proposed that [11], for the straight and parallel motion of a given fluid, the shear stress between two adjoining layers tangent to the direction of the flow, is proportional to the velocity gradient in a direction perpendicular to the layers. Mathematically,

$$\tau \propto \frac{\partial u}{\partial y},$$

or

$$\tau = \mu\frac{\partial u}{\partial y}, \tag{2.3.1}$$

where τ is the tangential stress (or viscous force) between the two layers, $\partial u/\partial y$ is the distance rate of change of velocity (i.e., the velocity gradient as $\delta y \to 0$) and μ is called the coefficient of viscosity.

Fluids that obey Newton's law of viscosity (2.3.1) are called *Newtonian* fluids. Fluids that behave differently are called *non-Newtonian* fluids - The viscosity of a non-Newtonian fluid changes with shear rate. Non-Newtonian fluids are classified as dilatents, pseudoplastics, and ideal plastics.

Although, viscosity changes with temperature (and with pressure, with little impact), it may be regarded as a constant for a particular temperature for Newtonian fluids. As fluid comes in contact with the solid boundary of the adjoining layers, it sticks to the boundary and its velocity relative to this boundary

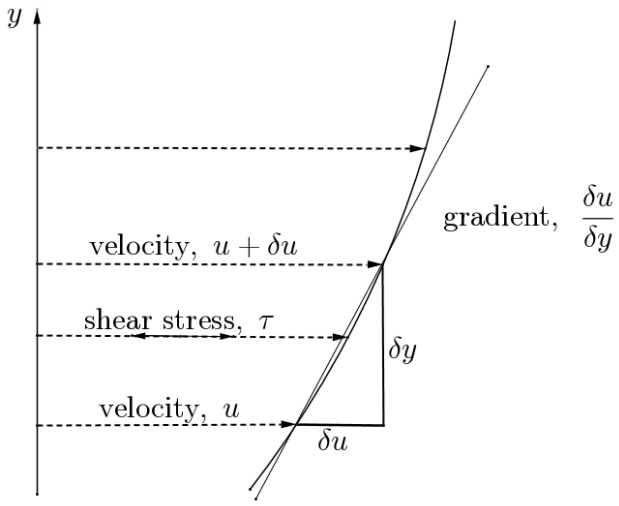

Figure 2.2: Fluid viscosity

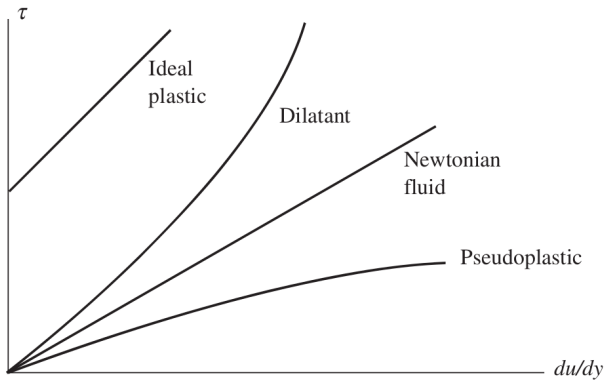

Figure 2.3: Newtonian and non-Newtonian fluid. [19]

becomes zero - any motion of the fluid would constitute an abrupt change. Hence, for a viscous liquid, a condition that there should be *no-slipping* at solid boundaries must be met. This condition is known as the *no-slip* condition. For blood, the *no-slip* condition is satisfied for blood particles as they come in contact with the wall of the artery.

2.4 Variable Viscosity

Blood can be seen as a suspension of red blood cells in plasma. Consider an incompressible flow of the blood such that the density ρ is uniform throughout. Viscosity, $\mu(r)$ however, varies as the blood flows in the radial direction. Einstein's model of variable viscosity is:

$$\mu(r) = \mu_0(1 + \lambda h(r)), \tag{2.4.1}$$

where μ_0 is the coefficient of viscosity of plasma, λ is a constant which takes the value 2.5 for blood (suspension of red blood cells which are considered to be of spherical shape) and $h(r)$ is the volume fraction of the red blood cells, known as hematocrit.

The analysis will be carried out using the following empirical formular for hematocrit [25]:

$$h(r) = H\left[1 - \left(\frac{r}{d_0}\right)^m\right], \tag{2.4.2}$$

and

$$H_r = \lambda H, \tag{2.4.3}$$

where H represents the maximum hematocrit at the mid line of the artery, m represents the parameter which determines the shape of the velocity profile of blood ($m \geq 2$) and H_r is the volumetric ratio of red blood cells in the blood and is known as the hematocrit parameter.

2.5 Governing Equations

Any fluid flow is governed by three basic laws namely: law of conservation of mass, law of conservation of energy, and law of conservation of momentum. These laws apply to a specified mass of the fluid and are expressed mathematically using the Lagrangian flow description. Let ρ be the fluid density, V the volume (system), $\Sigma\vec{F}$ the resultant force acting on the system, $\dot{Q}$ the time rate of energy change, $\dot{W}$ the time rate of work, $\vec{v}$ the velocity component of the flow and D/Dt the Lagrangian derivative following a fluid particle. Then, we state these three laws as follows:

- The law of conservation of mass states that, in a closed system, mass can neither be created nor destroyed. In other words, mass conservation law states that a quantity can neither be added nor removed from a system, hence, the mass of the system remains constant. Mathematically,

$$0 = \frac{D}{Dt}\int_{sys} \rho \mathrm{d}V. \tag{2.5.1}$$

- Let E denote the energy of the fluid system of mass m. We define E as follows:

$$E = me,$$

  where e is the heat energy density given by $(\rho c_p T)$, with c_p the heat capacity and T the absolute temperature.

  The law of conservation of energy states that the difference between the rate of heat transfer and the rate of work done by a system equals the rate of change of the energy E of the system. In essence, the energy applied to a system and the internal energy of the system are in equilibrium, so that energy remains constant. Mathematically,

$$\dot{Q} - \dot{W} = \frac{D}{Dt}\int_{sys} e\rho \mathrm{d}V. \tag{2.5.2}$$

- The law of conservation of momentum states that the algebraic sum of the forces acting on a system equals the rate of change of momentum of the system. Mathematically,

$$\Sigma\vec{F} = \frac{D}{Dt}\int_{sys} \vec{v}\rho \mathrm{d}V. \tag{2.5.3}$$

The law of conservation of energy and the law of conservation of momentum are respectively known as the first law of thermodynamics and Newton's second law.

2.6 Basic Assumptions

Let us consider blood flow through a porous medium in the axial direction of the artery with a symmetrically shaped mild stenosis inclined at an angle γ. Let ρ be the density of blood with variable viscosity μ. The artery has a finite length L.

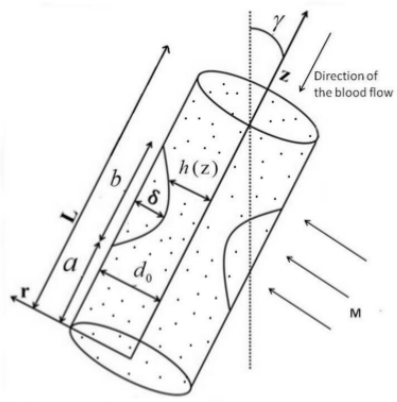

Figure 2.4: Geometry of an inclined non-tapered artery [25]

For our model, we make the following assumptions:

- **Geometry:** The artery is a circular cylindrical tube.
- **Fluid:** The blood is incompressible Newtonian fluid (the artery is large enough that a Newtonian model is appropriate [17]).
- **Flow:**
  - The flow is steady. This implies that the components of $\vec{v}$ and pressure p do not depend on time t.
  - The flow is in the axial direction and a uniform magnetic field (M) is applied in the radial direction (perpendicular to the flow). This implies that v_θ is zero and we are left with v_r and v_z. That is, $(r, \theta, z) = (r, 0, z)$.
  - The flow is axisymmetric. This implies that v_r, v_z and p do not depend on θ.

We assume that the blood is electrically conducting and is subjected to an electromagnetic (Lorentz) force. Consider the dimensionless magnetic Reynolds number defined by:

$$R_e = \sigma_1 \mu_m \times (\text{characteristic velocity}) \times (\text{characteristic length})$$

where σ_1 and μ_m are the electrical conductivity and magnetic permeability, respectively. We assume that R_e is small ($R_e \ll 1$) so that the induced magnetic field is negligible compared to the applied magnetic field [6]. The electric field $E_f = 0$ since the flow is not subjected to any applied voltage. The Lorentz force (or electromagnetic force) E_M is defined by:

$$E_M = J \times M, \tag{2.6.1}$$

where J is the electric current density defined by

$$J = \sigma_1(E_f + v_z \times M).$$

Hence,

$$E_M = \sigma_1(E_f + v_z \times M) \times M.$$

But the electric field $E_f = 0$. Also, M is related to the magnetic field strength H_0 by

$$M = \mu_m H_0.$$

Hence, (2.6.1) becomes

$$E_M = \sigma_1(v_z \times (\mu_m H_0)) \times (\mu_m H_0). \tag{2.6.2}$$

2.6.1 Reynolds Transport Theorem. Reynolds transport theorem is an analytical tool which enables us to shift from describing the laws governing fluid motion using the system concept to using the control volume concept, that is, a system-to-control-volume transformation.

A system is a specified collection of an identifiable quantity of fluid particles, while a control volume is a mass-dependent volume (considered fixed) in space.

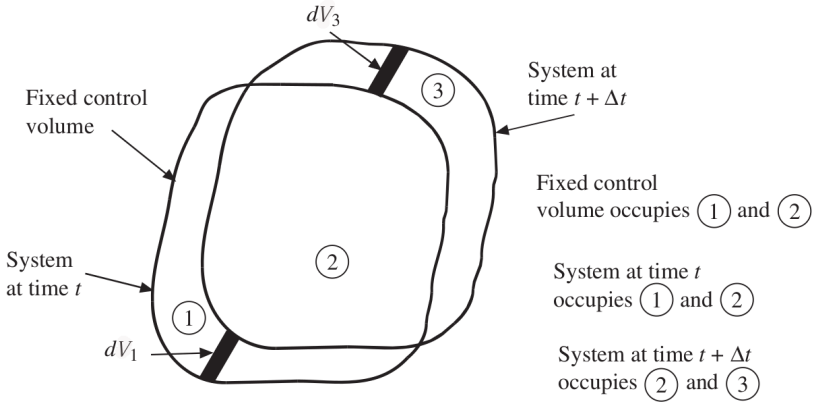

Figure 2.5: The system and the fixed control volume. [19]

Figure 2.5 illustrates the difference between system and control volume. It represents a general fixed volume at time t and at time $t + \Delta t$ in space, where Δt denotes a "small" change in time.

Let B be the amount of mass, momentum or energy contained in the total mass of a system or control volume.

Let β be the amount of B per unit mass.

That is,

$$\beta = \frac{B}{m}, \quad \text{and} \quad B = \beta \cdot m.$$

Then we have:

$$\begin{aligned} \frac{DB_{sys}}{Dt} &\cong \frac{B_{sys}(t + \Delta t) - B_{sys}(t)}{\Delta t} \\ &= \frac{B_3(t + \Delta t) + B_2(t + \Delta t) - B_1(t) - B_2(t)}{\Delta t} \end{aligned}$$

$$\frac{DB_{sys}}{Dt} \cong \frac{B_3(t+\Delta t)+B_2(t+\Delta t)-B_1(t)-B_2(t)+B_1(t+\Delta t)-B_1(t+\Delta t)}{\Delta t}$$
$$= \frac{B_2(t+\Delta t)+B_1(t+\Delta t)-B_2(t)-B_1(t)}{\Delta t}+\frac{B_3(t+\Delta t)-B_1(t+\Delta t)}{\Delta t}. \tag{2.6.3}$$

We note that the ratio

$$\frac{B_2(t+\Delta t)+B_1(t+\Delta t)-B_2(t)-B_1(t)}{\Delta t},$$

in (2.6.3), refers to the control volume which we denote as c.v for short, so that

$$\frac{B_2(t+\Delta t)+B_1(t+\Delta t)-B_2(t)-B_1(t)}{\Delta t} \cong \frac{\mathrm{d}B_{c.v}}{\mathrm{d}t} = \frac{d}{dt}\int_{c.v}\beta\rho \mathrm{d}V, \tag{2.6.4}$$

which is the time rate of B within the control volume.

The ratio

$$\frac{B_3(t+\Delta t)-B_1(t+\Delta t)}{\Delta t},$$

in (2.6.3), results from fluid flowing into volume ③ and out of volume ①.

If $\hat{n}$ is the outward unit normal everywhere on the control surface, then we define $\mathrm{d}V_1 = -\hat{n}\cdot\vec{v}\Delta t\mathrm{d}A_1$ and $\mathrm{d}V_3 = \hat{n}\cdot\vec{v}\Delta t\mathrm{d}A_3$, so that

$$B_3(t+\Delta t)-B_1(t+\Delta t) = \int_{V_3}\beta\rho\mathrm{d}V_3 - \int_{V_1}\beta\rho\mathrm{d}V_1 \tag{2.6.5}$$
$$= \int_{A_3}\beta\rho\hat{n}\cdot\vec{v}\Delta t\mathrm{d}A_3 + \int_{A_1}\beta\rho\hat{n}\cdot\vec{v}\Delta t\mathrm{d}A_1 \tag{2.6.6}$$
$$= \int_{c.s}\beta\rho\hat{n}\cdot\vec{v}\Delta t\mathrm{d}A, \tag{2.6.7}$$

where $A = A_1 + A_3$ surrounds the entire volume and c.s denotes the control surface surrounding the control volume.

Substituting (2.6.4) and (2.6.7) in (2.6.3), we obtain the Reynolds transport theorem:

$$\frac{DB_{sys}}{Dt} = \frac{d}{dt}\int_{c.v}\beta\rho\mathrm{d}V + \int_{c.s}\beta\rho\hat{n}\cdot\vec{v}\mathrm{d}A. \tag{2.6.8}$$

2.6.2 Continuity (Mass Conservation) Equation. Using the Reynolds transport theorem (2.6.8) with parameter $B = \text{mass}, m \implies \beta = 1$, and the law of conservation of mass (2.5.1), we obtain

$$0 = \frac{DM_{sys}}{Dt} = \frac{d}{dt}\int_{c.v}\rho\mathrm{d}V + \int_{c.s}\rho\hat{n}\cdot\vec{v}\mathrm{d}A,$$
$$\implies \int_{c.s}\rho\hat{n}\cdot\vec{v}\mathrm{d}A = -\frac{d}{dt}\int_{c.v}\rho\mathrm{d}V.$$

We assumed an incompressible fluid, that is, $\rho =$ constant and for a steady flow,

$$\int_{c.s}\rho\hat{n}\cdot\vec{v}\mathrm{d}A = 0,$$

which implies, by Gauss's theorem:

$$\int_{c.v}\nabla\cdot(\rho\vec{v})\mathrm{d}V = 0$$

$$\implies \rho \int_{c.v} \nabla \cdot \vec{v} \mathrm{d}V = 0$$
$$\implies \nabla \cdot \vec{v} = 0,$$

or

$$\frac{1}{r}\frac{\partial}{\partial r}(rv_r) + \frac{1}{r}\frac{\partial v_\theta}{\partial \theta} + \frac{\partial v_z}{\partial z} = 0,$$

and since there is no motion in θ-direction, the continuity equation becomes

$$\frac{\partial v_r}{\partial r} + \frac{v_r}{r} + \frac{\partial v_z}{\partial z} = 0. \tag{2.6.9}$$

2.6.3 Momentum Conservation Equations. The momentum equations result from the Newton's second law of motion, and are given in the radial and axial directions as follows:

- **Momentum Equation (r-direction):** Using the Reynolds transport theorem (2.6.8) with parameter B = momentum $(\vec{P}) = m\vec{v} \implies \beta = \vec{v}$, and the law of conservation of momentum (2.5.3), we obtain

  $$\Sigma \vec{F} = \frac{d}{dt}\int_{c.v} \vec{v}\rho \mathrm{d}V + \int_{c.s} \vec{v}\rho\vec{v}\cdot\hat{n}\mathrm{d}A.$$

  The force $\vec{F}$ consists of the gravity, centripetal, pressure and viscous forces. The gravity and centripetal forces are body forces (forces which act on the blood inside the containing volume), while the pressure and viscous forces are surface forces (forces which act on surface of the volume). That is,

  $$\Sigma \vec{F} = \int_{c.v} \rho\vec{g}_r \mathrm{d}V + \int_{c.v} \rho\omega^2 r \mathrm{d}V - \int_{c.s} p\hat{n}\mathrm{d}A + \int_{c.s} \tau_v \hat{n}\mathrm{d}A,$$

  where $\int_{c.v} \rho\vec{g}_r \mathrm{d}V$ is the gravity force with $\vec{g}_r$ the gravitational acceleration in direction r, $\int_{c.v} \rho\omega^2 r \mathrm{d}V$ is the centripetal force with $\omega = v_\theta/r$ the centripetal acceleration, $-\int_{c.s} p\hat{n}\mathrm{d}A$ is the pressure force with p the applied pressure, and $\int_{c.s} \tau_v\hat{n}\mathrm{d}A$ is the viscous force with τ_v the shear force.

  Hence, we write:

  $$\int_{c.v} \rho\vec{g}_r \mathrm{d}V + \int_{c.v} \rho\frac{v_\theta^2}{r}\mathrm{d}V - \int_{c.s} p\hat{n}\mathrm{d}A + \int_{c.s} \tau_v\hat{n}\mathrm{d}A = \frac{d}{dt}\int_{c.v} \vec{v}\rho\mathrm{d}V + \int_{c.s} \vec{v}\rho\vec{v}\cdot\hat{n}\mathrm{d}A.$$

  Applying Gauss's theorem, we have

  $$\int_{c.v} \rho\vec{g}_r \mathrm{d}V + \int_{c.v} \rho\frac{v_\theta^2}{r}\mathrm{d}V - \int_{c.v} \nabla p\mathrm{d}V + \int_{c.v} \nabla\tau_v\mathrm{d}V = \int_{c.v} \frac{\partial\vec{v}}{\partial t}\rho\mathrm{d}V + \int_{c.v} \vec{v}\cdot\nabla(\rho\vec{v})\mathrm{d}V.$$

  But, by Newton's law of viscosity (2.3.1), we have $\tau_v = \mu\nabla\vec{v}$. Hence, we obtain

  $$\int_{c.v} \left(\rho\frac{v_\theta^2}{r} + \rho\vec{g}_r - \nabla p + \mu\nabla^2\vec{v}\right)\mathrm{d}V = \int_{c.v} \left(\frac{\partial\vec{v}}{\partial t}\rho + \vec{v}\cdot\nabla(\rho\vec{v})\right)\mathrm{d}V.$$

  That is,

  $$\rho\left(\frac{\partial\vec{v}}{\partial t} + \vec{v}\cdot\nabla\vec{v}\right) = \rho\frac{v_\theta^2}{r} + \rho\vec{g}_r - \nabla p + \mu\nabla^2\vec{v},$$

  or

  $$\rho\left[v_r\frac{\partial v_r}{\partial r} + \frac{v_\theta}{r}\frac{\partial v_r}{\partial\theta} + v_z\frac{\partial v_r}{\partial z} + \frac{\partial v_r}{\partial z} + \frac{\partial\vec{v}}{\partial t}\right] = \rho\frac{v_\theta^2}{r} + \rho\vec{g_r} - \nabla p + \mu\nabla^2\vec{v}.$$

The density, ρ is assumed to be uniform, hence we realize that the gravitational force is immediately balanced by a pressure gradient $\nabla p_0 = \vec{g}_r$ which does not relate with any flow [8], and by defining $\bar{P} = p - p_0$, with other assumptions, we get the following

$$\rho\left[v_r\frac{\partial v_r}{\partial r} + \frac{v_\theta}{r}\frac{\partial v_r}{\partial \theta} + v_z\frac{\partial v_r}{\partial z} + \frac{\partial \vec{v}}{\partial t}\right] = \rho\frac{v_\theta^2}{r} - \frac{\partial \bar{P}}{\partial r} + \mu\left(\nabla^2 v_r - \frac{v_r}{r^2} - \frac{2}{r^2}\frac{\partial v_\theta}{\partial \theta}\right),$$

where

$$\nabla^2 v_r = \frac{\partial^2 v_r}{\partial r^2} + \frac{1}{r}\frac{\partial v_r}{\partial r} + \frac{1}{r^2}\frac{\partial^2 v_r}{\partial \theta^2} + \frac{\partial^2 v_r}{\partial z^2}.$$

Hence, with our assumptions, we get

$$\begin{aligned}
\rho\left[v_r\frac{\partial v_r}{\partial r} + v_z\frac{\partial v_r}{\partial z}\right] &= -\frac{\partial P}{\partial r} + \mu\left[\frac{\partial^2 v_r}{\partial r^2} + \frac{1}{r}\frac{\partial v_r}{\partial r} + \frac{\partial^2 v_r}{\partial z^2} - \frac{v_r}{r^2}\right] \\
&= -\frac{\partial P}{\partial r} + \mu\frac{\partial^2 v_r}{\partial r^2} + \frac{\mu}{r}\frac{\partial v_r}{\partial r} + \mu\frac{\partial^2 v_r}{\partial z^2} - \mu\frac{v_r}{r^2} \\
&= -\frac{\partial P}{\partial r} + 2\mu\frac{\partial^2 v_r}{\partial r^2} + 2\frac{\mu}{r}\frac{\partial v_r}{\partial r} - 2\mu\frac{v_r}{r^2} - \mu\frac{\partial^2 v_r}{\partial r^2} + \mu\frac{v_r}{r^2} - \frac{\mu}{r}\frac{\partial v_r}{\partial r} + \mu\frac{\partial^2 v_r}{\partial z^2} \\
&= -\frac{\partial P}{\partial r} + 2\mu\frac{\partial^2 v_r}{\partial r^2} + 2\frac{\mu}{r}\frac{\partial v_r}{\partial r} - 2\mu\frac{v_r}{r^2} - \mu\frac{\partial}{\partial r}\left(\frac{\partial v_r}{\partial r} + \frac{v_r}{r}\right) + \mu\frac{\partial^2 v_r}{\partial z^2} \\
&= -\frac{\partial P}{\partial r} + 2\mu\frac{\partial^2 v_r}{\partial r^2} + 2\frac{\mu}{r}\frac{\partial v_r}{\partial r} - 2\mu\frac{v_r}{r^2} + \mu\frac{\partial}{\partial r}\left(\frac{\partial v_z}{\partial z}\right) + \mu\frac{\partial^2 v_r}{\partial z^2} \\
&= -\frac{\partial P}{\partial r} + 2\mu\frac{\partial^2 v_r}{\partial r^2} + 2\frac{\mu}{r}\frac{\partial v_r}{\partial r} - 2\mu\frac{v_r}{r^2} + \mu\frac{\partial^2 v_z}{\partial z \partial r} + \mu\frac{\partial^2 v_r}{\partial z^2}.
\end{aligned}$$

Hence, the momentum equation in r-direction becomes

$$\rho\left[v_r\frac{\partial v_r}{\partial r} + v_z\frac{\partial v_r}{\partial z}\right] = -\frac{\partial \bar{P}}{\partial r} + \frac{\partial}{\partial r}\left[2\mu\frac{\partial v_r}{\partial r}\right] + 2\frac{\mu}{r}\left[\frac{\partial v_r}{\partial r} - \frac{v_r}{r}\right] + \frac{\partial}{\partial z}\left[\mu\left(\frac{\partial v_r}{\partial z} + \frac{\partial v_z}{\partial r}\right)\right]. \quad (2.6.10)$$

- **Momentum Equation (z-direction):** Similarly, the momentum equation in z-direction is

$$\rho\left(\frac{\partial \vec{v}}{\partial t} + \vec{v}\cdot\nabla\vec{v}\right) = \rho\vec{g}_z - \nabla p + \mu\nabla^2\vec{v} - E_M + F_B + \frac{\partial P}{\partial L},$$

or

$$\rho\left[v_r\frac{\partial v_z}{\partial r} + \frac{v_\theta}{r}\frac{\partial v_z}{\partial \theta} + v_z\frac{\partial v_z}{\partial z}\right] = \rho\vec{g}_z - \nabla p + \mu\left(\frac{\partial^2 v_z}{\partial r^2} + \frac{1}{r}\frac{\partial v_z}{\partial r} + \frac{1}{r^2}\frac{\partial^2 v_z}{\partial \theta^2} + \frac{\partial^2 v_z}{\partial z^2}\right) - E_M + F_B + \frac{\partial P}{\partial L},$$

where E_M is the electromagnetic force defined in (2.6.2), $F_B = \rho g\alpha(T - T_0)\cos\gamma$ is the buoyancy force per unit volume, with α a constant, known as the volumetric coefficient of thermal expansion, and $\partial P/\partial L = -(\mu v_z)/k_1$ is the pressure drop per unit length of the fluid with k_1 the permeability of the porous medium.

Knowing again that the density, ρ is assumed to be uniform, we realize the gravitational force is immediately balanced by a pressure gradient $\nabla p_0 = \vec{g}_z$ which does not relate with any flow [8], and by defining $\bar{P} = p - p_0$, with other assumptions, we have the following:

$$\rho\left[v_r\frac{\partial v_z}{\partial r} + v_z\frac{\partial v_z}{\partial z}\right] = -\frac{\partial \bar{P}}{\partial z} + \mu\frac{\partial^2 v_z}{\partial r^2} + \frac{\mu}{r}\frac{\partial v_z}{\partial r} + \mu\frac{\partial^2 v_z}{\partial z^2} - \sigma_1\mu_m^2 H_0^2 v_z + \rho g\alpha(T - T_0)\cos\gamma - \frac{\mu v_z}{k_1}$$

$$\begin{aligned}\rho\left[v_r\frac{\partial v_z}{\partial r}+v_z\frac{\partial v_z}{\partial z}\right] &= -\frac{\partial \bar{P}}{\partial z}+2\mu\frac{\partial^2 v_z}{\partial z^2}+\frac{\mu}{r}\frac{\partial v_r}{\partial z}-\mu\frac{\partial^2 v_z}{\partial z^2}+\mu\frac{v_r}{r^2}-\frac{\mu}{r}\frac{\partial v_r}{\partial z}+\frac{\mu}{r}\frac{\partial v_z}{\partial r}+\mu\frac{\partial^2 v_z}{\partial r^2}\\ &\quad -\sigma_1\mu_m^2H_0^2v_z+\rho g\alpha(T-T_0)\cos\gamma-\frac{\mu v_z}{k_1}\\ &= -\frac{\partial \bar{P}}{\partial z}+2\mu\frac{\partial^2 v_z}{\partial z^2}+\frac{\mu}{r}\frac{\partial v_r}{\partial z}+\mu\frac{\partial}{\partial z}\left(-\frac{\partial v_z}{\partial z}-\frac{v_r}{r}\right)+\frac{\mu}{r}\frac{\partial v_z}{\partial r}+\mu\frac{\partial^2 v_z}{\partial r^2}-\sigma_1\mu_m^2H_0^2v_z\\ &\quad +\rho g\alpha(T-T_0)\cos\gamma-\frac{\mu v_z}{k_1}\\ &= -\frac{\partial \bar{P}}{\partial z}+2\mu\frac{\partial^2 v_z}{\partial z^2}+\frac{\mu}{r}\frac{\partial v_r}{\partial z}+\mu\frac{\partial}{\partial z}\left(\frac{\partial v_r}{\partial r}\right)+\frac{\mu}{r}\frac{\partial v_z}{\partial r}+\mu\frac{\partial^2 v_z}{\partial r^2}-\sigma_1\mu_m^2H_0^2v_z\\ &\quad +\rho g\alpha(T-T_0)\cos\gamma-\frac{\mu v_z}{k_1}\end{aligned}$$

$$\begin{aligned}\rho\left[v_r\frac{\partial v_z}{\partial r}+v_z\frac{\partial v_z}{\partial z}\right] &= -\frac{\partial \bar{P}}{\partial z}+2\mu\frac{\partial^2 v_z}{\partial z^2}+\frac{\mu}{r}\frac{\partial v_r}{\partial z}+\mu\frac{\partial^2 v_r}{\partial r\partial z}+\frac{\mu}{r}\frac{\partial v_z}{\partial r}+\mu\frac{\partial^2 v_z}{\partial r^2}-\sigma_1\mu_m^2H_0^2v_z\\ &\quad +\rho g\alpha(T-T_0)\cos\gamma-\frac{\mu v_z}{k_1}.\end{aligned}$$

Hence, the momentum equation in z-direction becomes

$$\begin{aligned}\rho\left[v_r\frac{\partial v_z}{\partial r}+v_z\frac{\partial v_z}{\partial z}\right] &= -\frac{\partial \bar{P}}{\partial z}+\frac{\partial}{\partial z}\left[2\mu\frac{\partial v_z}{\partial z}\right]+\frac{1}{r}\frac{\partial}{\partial r}\left[\mu r\left(\frac{\partial v_r}{\partial z}+\frac{\partial v_z}{\partial r}\right)\right]-\sigma_1\mu_m^2H_0^2v_z\\ &\quad +\rho g\alpha(T-T_0)\cos\gamma-\frac{\mu v_z}{k_1}.\end{aligned}\tag{2.6.11}$$

2.6.4 Energy Equation. Using the Reynolds transport theorem (2.6.8) with parameter $B=E=me \implies \beta=e$, and the law of energy conservation (2.5.2), we obtain

$$\frac{d}{dt}\int_{c.v}e\rho\mathrm{d}V+\int_{c.s}e\rho\vec{v}\cdot\hat{n}\mathrm{d}A=\dot{Q}-\dot{W},$$

with the body heating rate $\dot{Q}=-\int_{c.s}(-k\nabla T)\cdot\hat{n}\mathrm{d}A$. Along the wall of the artery, the work rate term $\dot{W}$ is due to the arterial blood viscous stresses on the entire surface of the wall and we write $\dot{W}=\dot{W}_v$, where $\dot{W}_v$ is the viscous work rate. However, the *no-slip* condition at the wall of the artery implies $\vec{v}_b=0$, and $\dot{W}=\dot{W}_v=-\int_{c.s}\tau_b\vec{v}_b\mathrm{d}A=0$. Hence, we have

$$\int_{c.v}\frac{\partial e}{\partial t}\rho\mathrm{d}V+\int_{c.s}e\rho\vec{v}\cdot\hat{n}\mathrm{d}A=\int_{c.s}(k\nabla T)\cdot\hat{n}\mathrm{d}A,$$

and by Gauss's theorem, we have

$$\begin{aligned}\int_{c.v}\frac{\partial e}{\partial t}\rho\mathrm{d}V+\int_{c.v}\vec{v}\cdot\nabla(e\rho)\mathrm{d}V &= \int_{c.v}\nabla\cdot(k\nabla T)\mathrm{d}V\\ \int_{c.v}\rho c_p\left(\frac{\partial T}{\partial t}+\vec{v}\cdot\nabla T\right)\mathrm{d}V &= \int_{c.v}(k\nabla^2T)\mathrm{d}V\\ \implies \rho c_p\left(\frac{\partial T}{\partial t}+\vec{v}\cdot\nabla T\right) &= k\nabla^2T\\ \rho c_p\left[v_r\frac{\partial T}{\partial r}+\frac{v_\theta}{r}\frac{\partial T}{\partial\theta}+v_z\frac{\partial T}{\partial z}+\frac{\partial T}{\partial t}\right] &= k\left[\frac{\partial^2T}{\partial r^2}+\frac{1}{r}\frac{\partial T}{\partial r}+\frac{1}{r^2}\frac{\partial^2T}{\partial\theta^2}+\frac{\partial^2T}{\partial z^2}\right].\end{aligned}\tag{2.6.12}$$

Consider the function Φ_v called the viscous dissipation function - the rate at which the work done against viscous forces in the form of kinetic energy, is converted by an irreversible process, into internal energy of the blood. Φ_v is defined by [21]

$$\begin{aligned}\Phi_v =& 2\mu\left[\left(\frac{\partial v_r}{\partial r}\right)^2+\left(\frac{1}{r}\frac{\partial v_\theta}{\partial \theta}+\frac{v_r}{r}\right)^2+\left(\frac{\partial v_z}{\partial z}\right)^2\right]+\mu\left[r\frac{\partial}{\partial r}\left(\frac{v_\theta}{r}\right)+\frac{1}{r}\frac{\partial v_r}{\partial \theta}\right]^2\\&+\mu\left[\frac{1}{r}\frac{\partial v_z}{\partial \theta}+\frac{\partial v_\theta}{\partial z}\right]^2+\mu\left[\frac{\partial v_r}{\partial z}+\frac{\partial v_z}{\partial r}\right]^2-\frac{2}{3}\mu(\nabla\cdot\vec{v})^2.\end{aligned}$$

There is no motion in θ-direction and $\nabla\cdot\vec{v}=0$, hence, we have

$$\Phi_v = 2\mu\left[\left(\frac{\partial v_r}{\partial r}\right)^2+\left(\frac{v_r}{r}\right)^2+\left(\frac{\partial v_z}{\partial z}\right)^2\right]+\mu\left(\frac{\partial v_r}{\partial z}+\frac{\partial v_z}{\partial r}\right)^2.$$

Also, the blood transports heat energy as it flows in and out of the control volume, hence, we introduce the term $-Q_p(T-T_0)$, where Q_p is a dimensional heat parameter defined as blood perfusion mass flow rate times the specific heat of blood, T is the local temperature of the blood, and T_0 is the temperature of the blood at the stenotic region.

Adding these extra energy terms to (2.6.12), we obtain

$$\begin{aligned}\rho c_p\left[v_r\frac{\partial T}{\partial r}+\frac{v_\theta}{r}\frac{\partial T}{\partial \theta}+v_z\frac{\partial T}{\partial z}+\frac{\partial T}{\partial t}\right] =& k\left[\frac{\partial^2 T}{\partial r^2}+\frac{1}{r}\frac{\partial T}{\partial r}+\frac{1}{r^2}\frac{\partial^2 T}{\partial \theta^2}+\frac{\partial^2 T}{\partial z^2}\right]+2\mu\left[\left(\frac{\partial v_r}{\partial r}\right)^2+\left(\frac{v_r}{r}\right)^2+\left(\frac{\partial v_z}{\partial z}\right)^2\right]\\&+\mu\left(\frac{\partial v_r}{\partial z}+\frac{\partial v_z}{\partial r}\right)^2-Q_p(T-T_0),\\ \rho c_p\left[v_r\frac{\partial T}{\partial r}+v_z\frac{\partial T}{\partial z}\right] =& k\left[\frac{1}{r}\frac{\partial}{\partial r}\left(r\frac{\partial T}{\partial r}\right)+\frac{\partial^2 T}{\partial z^2}\right]+2\mu\left[\left(\frac{\partial v_r}{\partial r}\right)^2+\left(\frac{v_r}{r}\right)^2+\left(\frac{\partial v_z}{\partial z}\right)^2\right]\\&+\mu\left(\frac{\partial v_r}{\partial z}+\frac{\partial v_z}{\partial r}\right)^2-Q_p(T-T_0),\end{aligned}$$

or

$$\begin{aligned}\rho c_p\left[v_r\frac{\partial T}{\partial r}+v_z\frac{\partial T}{\partial z}\right] =& \frac{k}{r}\frac{\partial}{\partial r}\left(r\frac{\partial T}{\partial r}\right)+k\frac{\partial^2 T}{\partial z^2}+2\mu\left[\left(\frac{\partial v_r}{\partial r}\right)^2+\left(\frac{v_r}{r}\right)^2+\left(\frac{\partial v_z}{\partial z}\right)^2\right]\\&+\mu\left(\frac{\partial v_r}{\partial z}+\frac{\partial v_z}{\partial r}\right)^2-Q_p(T-T_0).\end{aligned}\tag{2.6.13}$$

2.7 Mathematical Formulation

Consider a tapered stenosed porous artery inclined at an angle γ with an externally applied magnetic field (M) as shown in Figure 2.6.

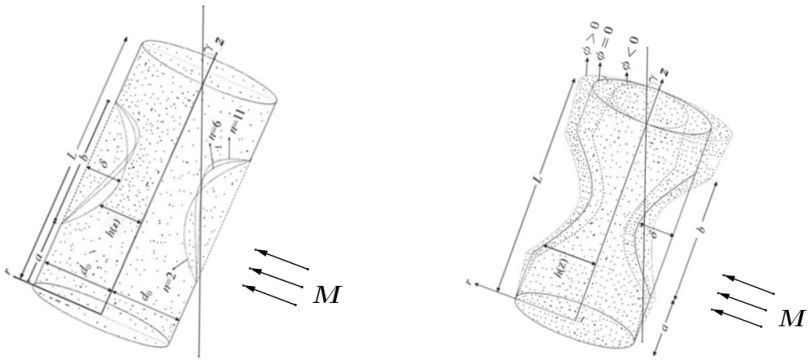

(a) Geometry of the axisymmetric stenosis in a porous artery. [15]

(b) Geometry of the tapered stenosed porous artery for different tapering angles. [15]

Figure 2.6: Schematic diagram for the geometry of the tapered porous artery with axisymmetric stenosis inclined at an angle γ.

Let $d(z)$ be the radius of the tapered artery in the region of stenosis, with [25]:

$$d(z) = d_0 + \xi z,$$

then, the geometry of the stenosis in dimensionless form is defined by [13, 25]:

$$h(z) = \begin{cases} d(z)\left[1 - \eta\left(b^{n-1}(z-a) - (z-a)^n\right)\right], & a \le z \le a+b, \\ d(z), \quad \text{otherwise}, \end{cases} \tag{2.7.1}$$

where d_0 is the radius of the non-tapered artery in the non-stenotic region, n is a parameter which determines the shape of the constriction profile ($n = 2$ for a symmetrically shaped stenosis and $n \ge 2$ for a non symmetric stenosis), b is the length of the stenosis and ξ is the tapering parameter defined by $\xi = \tan\phi$, where ϕ is the tapered angle which assumes value $\phi < 0$, $\phi > 0$ and $\phi = 0$ in the converging, diverging and non-tapered regions, respectively.

Let δ be the maximum height of the stenosis at the location: [25]

$$z = a + \frac{b}{n^{\frac{n}{n-1}}}, \tag{2.7.2}$$

then, we define the parameter η in (2.7.1) by: [25]

$$\eta = \frac{\delta n^{\frac{n}{n-1}}}{d_0 b^n (n-1)}.$$

Equations (2.6.9), (2.6.10), (2.6.11) and (2.6.13) are dimensional equations of motion which govern the flow of blood in the stenosed artery under the effect of magnetic field and heat transfer. These equations are not easy to solve by the number of parameters they include. This number of parameters, however, can be reduced by introducing non-dimensional groups.

We therefore introduce the following non-dimensional variables into (2.6.9), (2.6.10), (2.6.11) and

(2.6.13) to get the equivalent non-dimensional equations of motion [25]:

$$\begin{cases} v_r = \frac{uu_0\delta}{b}, \quad r = r'd_0, \quad z = z'b, \quad v_z = w'u_0, \quad h = h'd_0, \\ \bar{P} = \frac{u_0 b\mu_0 P}{d_0^2}, \quad R_e = \frac{\rho b u_0}{\mu_0}, \quad \Theta = \frac{T-T_0}{T_0}, \quad P_r = \frac{\mu c_p}{k}, \quad E_c = \frac{u_0^2}{c_p T_0}, \\ Z = \frac{k_1}{d_0^2}, \quad M^2 = \frac{\sigma H_0^2 d_0^2}{\mu_0}, \quad Q = \frac{Q_p d_0^2}{k}, \quad G_r = \frac{g\alpha d_0^3 T_0}{\nu^2}. \end{cases} \tag{2.7.3}$$

where R_e, P_r, E_c, G_r, Θ, Z, M, and Q respectively represent the Reynolds number, Prandtl number, Eckert number, Grashof number, temperature parameter, porosity parameter, magnetic field parameter and dimensionless heat source parameter. The term $\nu = \mu_0/\rho$ is the dynamic viscosity, α is the coefficient of thermal expansion, and k_1 is the permeability of the porous medium.

In order to adopt simple notations, we will drop the prime $'$ on r, z, w and h. This basically changes nothing since we now have them in their dimensionless forms and by considering $d_0 = 1$.

We assumed a symmetrically shaped mild stenosis in which case we have

$$\frac{\delta}{d_0} \ll 1, \tag{2.7.4}$$

and the conditions [25, 26]

$$\frac{R_e \delta n^{\frac{1}{n-1}}}{b} \ll 1, \tag{2.7.5}$$

$$d_0 n^{\frac{1}{n-1}} \sim \mathcal{O}(1), \tag{2.7.6}$$

then, the pressure gradient in the r-direction is negligible compared to the pressure gradient in the z-direction, that is,

$$\frac{\partial P}{\partial r} \ll \frac{\partial P}{\partial z}.$$

Also, condition (2.7.4) implies $\frac{\partial v_r}{\partial z} \ll 1$. Therefore, given the conditions (2.7.4), (2.7.5), (2.7.6), the *no-slip* boundary condition, and that $h(z)$, defined in (2.7.1), is the geometry of the stenosis in non-dimensional form, then (2.6.9), (2.6.10), (2.6.11), and (2.6.13) in their non-dimensional forms become

- Continuity Equation

$$\frac{\partial v_z}{\partial z} = 0. \tag{2.7.7}$$

- Momentum Equation (r-direction)

$$\frac{\partial P}{\partial r} = 0. \tag{2.7.8}$$

- Momentum Equation (z-direction)

  From (2.4.2) and the non-dimensional group (2.7.3), taking $\mu_0 = \mu_m = 1$, and with $d_0 = 1$, we obtain the following:

$$\begin{cases} \mu = \mu_0 \left(1 + H_r \left[1 - r^m\right]\right) \implies \frac{\partial \mu}{\partial r} = -H_r m r^{m-1}, \\ \sigma_1 = \frac{M^2\mu_0}{H_0^2 d_0^2} = \frac{M^2\mu_0}{H_0^2}, \\ k_1 = d_0^2 Z = Z, \\ T_0 = \frac{\nu^2 G_r}{g\alpha} \implies T - T_0 = \Theta T_0 = \Theta \frac{\nu^2 G_r}{g\alpha}. \end{cases} \tag{2.7.9}$$

Putting (2.7.9) in (2.6.11), we obtain the following:

$$\begin{aligned}
\frac{\partial P}{\partial z} &= \frac{1}{r}\frac{\partial}{\partial r}\left(\mu r\frac{\partial w}{\partial r}\right) - \frac{M^2\mu_0}{H_0^2}H_0^2 w + \rho g\alpha\Theta\frac{\nu^2 G_r}{g\alpha}\cos\gamma - \frac{\mu w}{Z} \\
&= \frac{\partial\mu}{\partial r}\frac{\partial w}{\partial r} + \frac{\mu}{r}\frac{\partial w}{\partial r} + \mu\frac{\partial}{\partial r}\left(\frac{\partial w}{\partial r}\right) - M^2 w - \left(1 + H_r\left(1 - r^m\right)\right)\frac{w}{Z} + G_r\Theta\cos\gamma \quad [\mu_0^2/\rho \text{ taken as } 1] \\
&= -H_r m r^{m-1}\frac{\partial w}{\partial r} + \left[\frac{1}{r} + H_r\left(\frac{1}{r} - r^{m-1}\right)\right]\frac{\partial w}{\partial r} + \left[1 + H_r(1 - r^m)\right]\frac{\partial}{\partial r}\left(\frac{\partial w}{\partial r}\right) \\
&\quad - w\left(M^2 + \frac{1}{Z} + \frac{H_r}{Z}(1 - r^m)\right) + G_r\Theta\cos\gamma \\
&= \left[\frac{1}{r} + H_r\left(\frac{1}{r} - r^{m-1}\right) - H_r m r^{m-1}\right]\frac{\partial w}{\partial r} + \left[1 + H_r(1 - r^m)\right]\frac{\partial}{\partial r}\left(\frac{\partial w}{\partial r}\right) \\
&\quad - w\left(M^2 + \frac{1}{Z} + \frac{H_r}{Z}(1 - r^m)\right) + G_r\Theta\cos\gamma
\end{aligned}$$

that is, the momentum equation in dimensionless form is:

$$\begin{aligned}
\frac{\partial P}{\partial z} &= \left[\frac{1}{r} + H_r\left(\frac{1}{r} - (m+1)r^{m-1}\right)\right]\frac{\partial w}{\partial r} + \left[1 + H_r(1 - r^m)\right]\frac{\partial}{\partial r}\left(\frac{\partial w}{\partial r}\right) \\
&\quad - w\left(M^2 + \frac{1}{Z} + \frac{H_r}{Z}(1 - r^m)\right) + G_r\Theta\cos\gamma.
\end{aligned} \tag{2.7.10}$$

- Energy Equation

  From the non-dimensional group (2.7.3), taking $\mu_0 = u_0 = 1$, and with $d_0 = 1$, we obtain the following:

$$\begin{cases}
T = T_0\Theta + T_0 \implies \frac{\partial}{\partial r}\left(r\frac{\partial T}{\partial r}\right) = T_0\frac{\partial}{\partial r}\left(r\frac{\partial\Theta}{\partial r}\right) \\
\frac{1}{c_p} = \frac{E_c T_0}{u_0^2} \implies \mu = \frac{k}{c_p}P_r = kT_0E_cP_r, \\
Q_p = kQ \implies Q_p(T - T_0) = kT_0Q\Theta.
\end{cases} \tag{2.7.11}$$

  where, $B_r = E_cP_r$ is the ratio of the heat produced by viscous dissipation to that transported by molecular conduction, i.e., the ratio between viscous heat generation and external heating.

  Putting (2.7.11) in (2.6.13), we get the following:

$$0 = \frac{k}{r}T_0\frac{\partial}{\partial r}\left(r\frac{\partial\Theta}{\partial r}\right) + kT_0E_cP_r\left(\frac{\partial w}{\partial r}\right)^2 - kT_0Q\Theta,$$

  and dividing through by kT_0, we obtain the dimensionless energy equation:

$$\frac{1}{r}\frac{\partial}{\partial r}\left(r\frac{\partial\Theta}{\partial r}\right) + E_cP_r\left(\frac{\partial w}{\partial r}\right)^2 - Q\Theta = 0. \tag{2.7.12}$$

To solve the momentum and energy equations (2.7.10) and (2.7.12), we use the axisymmetric boundary conditions of the flow axial velocity at the mid line of the artery:

$$\frac{\partial w}{\partial r} = 0, \quad \frac{\partial\Theta}{\partial r} = 0 \quad at \quad r = 0, \tag{2.7.13}$$

and the *no-slip* boundary conditions at the wall of the artery:

$$w = 0, \quad \Theta = 0, \quad at \quad r = h(z), \tag{2.7.14}$$

where $h(z)$, defined by

$$h(z) = (1 + \xi' z)[1 - \eta'((z - a') - (z - a')^n)] \quad \text{when} \quad a' \leq z \leq a' + 1, \tag{2.7.15}$$

is the geometry of the stenosis when the radius d_0 of the artery is of unit length.

In (2.7.15), η', a' and ξ' are defined as follows:

$$\eta' = \frac{\delta' n^{\frac{n}{n-1}}}{(n-1)} \text{ with } \delta' = \frac{\delta}{d_0}, \quad a' = \frac{a}{b}, \quad \xi' = \frac{\xi b}{d_0}.$$

3. Differential Transform Method (DTM)

3.1 Introduction

In mathematics and nature, we come up with problems which are essentially nonlinear. These problems can be solved through analytical or numerical approach. In the past years, many analytical methods have been presented for solving nonlinear problems, some of which are the [27] Homotopy Analysis Method (HAM), Homotopy Perturbation Method (HPM), Adonian Decomposition Method (ADM), Weighted Residual Method (WRM), etc.

The Differential Transform Method (DTM) is one of the numerical methods for solving differential and integral equations. The method was first introduced by Zhou [27] who used it to solve linear and nonlinear electrical circuits problem, and since then, many scientists have developed immense interests in the applications of the DTM to solve various scientific problems.

The DTM is based on the Taylor series expansion of a function and is indeed, an alternative method for obtaining analytic Taylor series solution of differential equations. One major advantage of the DTM is that it can be used to solve nonlinear differential equations without going through the process of linearization and discretization, hence, errors due to discretization are inherently avoided by the DTM.

In this chapter, we will present the principle of Differential Transform Method for solving differential equations, and use it to solve the energy and momentum equations (2.7.12) and (2.7.10).

3.2 Principle of Differential Transform Method (DTM)

In order for us to understand the concept of DTM, we suppose that a function $f(x)$ is analytic in a domain D, and that x_i is any point in the domain. The Taylor series expansion of $f(x)$ near $x = x_i$ is defined by

$$f(x) = \sum_{k=0}^{\infty} \frac{(x - x_i)^k}{k!} f^{(k)}(x_i), \tag{3.2.1}$$

where $f^{(k)}(x_i)$ represents the k-th derivative of $f(x)$ at $x = x_i$.

By taking $x_i = 0$, we obtain the Maclaurin series:

$$f(x) = \sum_{k=0}^{\infty} \frac{x^k}{k!} f^{(k)}(0). \tag{3.2.2}$$

3.2.1 Definition (Differential Transform of $f(x)$)**.** The differential transform of the function $f(x)$ at the point $x = 0$ is defined as follows:

$$F(k) = \frac{H^k}{k!} f^{(k)}(0), \tag{3.2.3}$$

where $F(k)$ is the transformed function and $f(x)$ is the original function. The differential spectrum of $F(k)$ is defined in the interval $x \in [0, H]$, where H is a constant whose value is mostly taken to be 1.

3.2.2 Definition (Differential Inverse Transform of $F(k)$)**.** The differential inverse transform of $F(k)$ is defined as follows:

$$f(x) = \sum_{k=0}^{\infty} \left(\frac{x}{H}\right)^k F(k). \tag{3.2.4}$$

In real applications, the function $f(x)$ is expressed by a finite series, hence, we write (3.2.4) as:

$$f(x) = \sum_{k=0}^{n} \left(\frac{x}{H}\right)^k F(k). \tag{3.2.5}$$

Some important mathematical operations resulting from definitions (3.2.1) and (3.2.2) are presented in the following theorems [24], and will be used in the next session to solve our blood flow model equations (2.7.10) and (2.7.12):

3.2.3 Theorem. *If $f(x) = \alpha u(x) \pm \beta v(x)$, then*

$$F(k) = \alpha U(k) \pm \beta V(k). \tag{3.2.6}$$

where α and β are constants.

3.2.4 Theorem. *If $f(x) = \frac{\partial^r}{\partial x^r} u(x)$, then for r an integer,*

$$F(k) = (k+1)(k+2)\cdots(k+r)U(k+r). \tag{3.2.7}$$

3.2.5 Theorem. *If $f(x) = u(x)v(x)$, then*

$$F(k) = \sum_{l=0}^{k} U(l)V(k-l). \tag{3.2.8}$$

3.2.6 Theorem. *If $f(x) = x^r$, then for r an integer,*

$$F(k) = \delta(k-r) = \begin{cases} 1, & \text{if } k = r, \\ 0, & \text{if } k \neq r. \end{cases} \tag{3.2.9}$$

3.3 Solution using DTM

Let the differential transform of $w(r)$ and $\Theta(r)$ be $W(k)$ and $G(k)$, respectively. We write the momentum equation (2.7.10) and the energy equation (2.7.12) respectively as follows:

$$\begin{aligned}(1+H_r)r^{-1}\frac{\partial w}{\partial r} - H_r(m+1)r^{m-1}\frac{\partial w}{\partial r} + (1+H_r)\frac{\partial^2 w}{\partial r^2} - H_r r^m \frac{\partial^2 w}{\partial r^2} \\ - \left(M^2 + \frac{1}{Z} + \frac{H_r}{Z}\right) w + \frac{H_r}{Z} r^m w + G_r \Theta \cos\gamma - \frac{\partial P}{\partial z} = 0,\end{aligned}$$

and

$$r^{-1}\frac{\partial \Theta}{\partial r} + \frac{\partial^2 \Theta}{\partial r^2} + E_c P_r \left(\frac{\partial w}{\partial r}\right)^2 - Q\Theta = 0,$$

and obtain their respective differential transforms as follows, using the theorems in section 3.2:

$$(1+H_r)\sum_{l=0}^{k}\delta(k-l+1)(l+1)W(l+1)-H_r(m+1)\sum_{l=0}^{k}\delta(k-l-m+1)(l+1)W(l+1)$$
$$+(1+H_r)(k+1)(k+2)W(k+2)-H_r\sum_{l=0}^{k}\delta(k-l-m)(l+1)(l+2)W(l+2)$$
$$-\left(M^2+\frac{1}{Z}+\frac{H_r}{Z}\right)W(k)+\frac{H_r}{Z}\sum_{l=0}^{k}\delta(k-l-m)W(l)+G_r\cos\gamma G(k)-\frac{\partial P}{\partial z}\delta(k)=0, \quad (3.3.1)$$

and

$$\sum_{l=0}^{k}\delta(k-l+1)(l+1)G(l+1)+(k+1)(k+2)G(k+2)$$
$$+E_cP_r\sum_{l=0}^{k}(k-l+1)W(k-l+1)(l+1)W(l+1)-QG(k)=0. \quad (3.3.2)$$

Applying equation (3.2.3) in the boundary conditions, taking $H=1$, we find that

$$W(0)=\frac{1}{0!}w(h(z))=a_1, \qquad G(0)=\frac{1}{0!}\Theta(h(z))=a_2,$$
$$W(1)=\frac{1}{1!}w'(0)=0, \qquad G(1)=\frac{1}{1!}\Theta'(0)=0.$$

where a_1 and a_2 are constants which can be determined by using the boundary conditions (2.7.14).

From (3.3.1), we obtain:

$$W(k+2)=\frac{H_r}{(1+H_r)(k+1)(k+2)}(m+1)\sum_{l=0}^{k}\delta(k-l-m+1)(l+1)W(l+1)$$
$$+\frac{\delta(k)}{(1+H_r)(k+1)(k+2)}\frac{\partial P}{\partial z}+\frac{W(k)}{(1+H_r)(k+1)(k+2)}\left(M^2+\frac{1}{Z}+\frac{H_r}{Z}\right)$$
$$+\frac{H_r}{(1+H_r)(k+1)(k+2)}\sum_{l=0}^{k}\delta(k-l-m)(l+1)(l+2)W(l+2)$$
$$-\frac{G_r\cos\gamma G(k)}{(1+H_r)(k+1)(k+2)}-\frac{H_r}{Z(1+H_r)(k+1)(k+2)}\sum_{l=0}^{k}\delta(k-l-m)W(l), \quad (3.3.3)$$

and from (3.3.2), we obtain

$$G(k+2)=\frac{QG(k)}{(k+1)(k+2)}-\frac{1}{(k+1)(k+2)}\sum_{l=0}^{k}\delta(k-l+1)(l+1)G(l+1)$$
$$-\frac{E_cP_r}{(k+1)(k+2)}\sum_{l=0}^{k}\delta(k-l+1)W(k-l+1)(l+1)W(l+1). \quad (3.3.4)$$

From (3.3.3) and (3.3.4), and taking $m=2$, we get the following iterations:

For $k = 0$,

$$\begin{aligned} W(2) &= \frac{\left(M^2 + \frac{1}{Z} + \frac{H_r}{Z}\right) W(0) - G_r \cos\gamma G(0) + \frac{\partial P}{\partial z}}{2(1+H_r)} \\ &= \frac{a_1}{2(1+H_r)}\left(M^2 + \frac{1}{Z} + \frac{H_r}{Z}\right) - \frac{G_r \cos\gamma}{2(1+H_r)} a_2 + \frac{1}{2(1+H_r)}\frac{\partial P}{\partial z}, \\ G(2) &= \frac{QG(0) - E_c P_r W(1)^2}{2} = \frac{Qa_2}{2}. \end{aligned}$$

For $k = 1$,

$$\begin{aligned} W(3) &= \frac{H_r(m+1)}{6(1+H_r)}\delta(2-m)W(1) + \frac{W(1)}{6(1+H_r)}\left(M^2 + \frac{1}{Z} + \frac{H_r}{Z}\right) - \frac{G_r \cos\gamma G(1)}{6(1+H_r)} = 0, \\ G(3) &= \frac{QG(1) - E_c P_r \left[2W(2)W(1) + 2W(1)W(2)\right]}{6} = \frac{QG(1) - 4E_c P_r W(1)W(2)}{6} = 0. \end{aligned}$$

For $k = 2$,

$$\begin{aligned} W(4) &= \frac{H_r(m+1)}{12(1+H_r)}\left[\delta(3-m)W(1) + 2\delta(2-m)W(2)\right] + \frac{H_r}{6(1+H_r)}\delta(2-m)W(2) \\ &\quad + \frac{W(2)}{12(1+H_r)}\left(M^2 + \frac{1}{Z} + \frac{H_r}{Z}\right) - \frac{H_r}{12Z(1+H_r)}\delta(2-m)W(0) - \frac{G_r \cos\gamma G(2)}{12(1+H_r)} \\ &= \frac{1}{24(1+H_r)^2}\left[a_1\left(M^2 + \frac{1}{Z} + H_r\frac{1}{Z}\right) - a_2 G_r \cos\gamma + \frac{\partial P}{\partial z}\right] \cdot \left[8H_r + M^2 + \frac{1}{Z} + H_r\frac{1}{Z}\right] \\ &\quad - a_1 H_r \frac{1}{Z} - \frac{1}{2}Qa_2 G_r \cos\gamma, \end{aligned}$$

$$\begin{aligned} G(4) &= \frac{QG(2) - E_c P_r \left[6W(3)W(1) + 4W(2)^2\right]}{12} \\ &= \frac{Q^2 a_2}{24} - \frac{E_c P_r}{12(1+H_r)^2}\left[a_1\left(M^2 + \frac{1}{Z} + \frac{H_r}{Z}\right) + \frac{\partial P}{\partial z} - a_2 G_r \cos\gamma\right]^2. \end{aligned}$$

For $k = 3$,

$$\begin{aligned} W(5) &= \frac{H_r(m+1)}{20(1+H_r)}\left[\delta(4-m)W(1) + 2\delta(3-m)W(2) + 3\delta(2-m)W(3)\right] \\ &\quad + \frac{H_r}{20(1+H_r)}\left[2\delta(3-m)W(2) + 6\delta(2-m)W(3)\right] + \frac{W(3)}{20(1+H_r)}\left(M^2 + \frac{1}{Z} + \frac{H_r}{Z}\right) \\ &\quad - \frac{H_r}{20Z(1+H_r)}\left[\delta(3-m)W(0) + \delta(2-m)W(1)\right] - \frac{G_r \cos\gamma G(3)}{20(1+H_r)} = 0 \\ G(5) &= \frac{QG(3) - E_c P_r \left[8W(4)W(1) + 12W(3)W(2)\right]}{20} = 0. \end{aligned}$$

Hence,

$$w(r) = a_1 + \left\{ \frac{a_1}{2(1+H_r)} \left(M^2 + \frac{1}{Z} + \frac{H_r}{Z} \right) - \frac{G_r \cos\gamma}{2(1+H_r)} a_2 + \frac{1}{2(1+H_r)} \frac{\partial P}{\partial z} \right\} r^2 + \left\{ \frac{1}{24(1+H_r)^2} \left[a_1 \left(M^2 + \frac{1}{Z} + H_r \frac{1}{Z} \right) - a_2 G_r \cos\gamma + \frac{\partial P}{\partial z} \right] \cdot \left[8H_r + M^2 + \frac{1}{Z} + H_r \frac{1}{Z} \right] - a_1 H_r \frac{1}{Z} - \frac{1}{2} Q a_2 G_r \cos\gamma \right\} r^4, \tag{3.3.5}$$

$$\Theta(r) = a_2 + \frac{Q a_2}{2} r^2 + \left\{ \frac{Q^2 a_2}{24} - \frac{E_c P_r}{12(1+H_r)^2} \left[a_1 \left(M^2 + \frac{1}{Z} + \frac{H_r}{Z} \right) + \frac{\partial P}{\partial z} - a_2 G_r \cos\gamma \right]^2 \right\} r^4. \tag{3.3.6}$$

The boundary conditions (2.7.14) imply:

$$w(h(z)) = a_1 + \left\{ \frac{a_1}{2(1+H_r)} \left(M^2 + \frac{1}{Z} + \frac{H_r}{Z} \right) - \frac{G_r \cos\gamma}{2(1+H_r)} a_2 + \frac{1}{2(1+H_r)} \frac{\partial P}{\partial z} \right\} h^2 + \left\{ \frac{1}{24(1+H_r)^2} \left[a_1 \left(M^2 + \frac{1}{Z} + H_r \frac{1}{Z} \right) - a_2 G_r \cos\gamma + \frac{\partial P}{\partial z} \right] \cdot \left[8H_r + M^2 + \frac{1}{Z} + H_r \frac{1}{Z} \right] - a_1 H_r \frac{1}{Z} - \frac{1}{2} Q a_2 G_r \cos\gamma \right\} h^4 = 0, \tag{3.3.7}$$

$$\Theta(h(z)) = a_2 + \frac{Q a_2}{2} h^2 + \left\{ \frac{Q^2 a_2}{24} - \frac{E_c P_r}{12(1+H_r)^2} \left[a_1 \left(M^2 + \frac{1}{Z} + \frac{H_r}{Z} \right) + \frac{\partial P}{\partial z} - a_2 G_r \cos\gamma \right]^2 \right\} h^4 = 0. \tag{3.3.8}$$

The Wolfram Mathematica 11.3 software is used to solve (3.3.7) and (3.3.8) simultaneously for a_1 and a_2. The values obtained for a_1 and a_2 are then substituted into (3.3.5) and (3.3.6) to have expressions for the velocity, $w(r)$ and temperature, $\Theta(r)$ which were then used to simulate velocity and temperature profiles. The expressions are not shown due to their lengths.

3.4 Volumetric Flow Rate

The volumetric flow rate, Q_v is defined as

$$Q_v = 2\pi \int_0^h r w \mathrm{d}r, \tag{3.4.1}$$

where w is the obtained axial velocity and r is the artery radius.

Substituting (3.3.5) into (3.4.1), and integrating, we obtain

$$Q_v = a_1 \pi h^2 + \left\{ \frac{a_1 \pi}{4(1+H_r)} \left(M^2 + \frac{1}{Z} + \frac{H_r}{Z} \right) - \frac{\pi G_r \cos\gamma}{4(1+H_r)} a_2 + \frac{\pi}{4(1+H_r)} \frac{\partial P}{\partial z} \right\} h^4 + \left\{ \frac{\pi}{72(1+H_r)^2} \left[a_1 \left(M^2 + \frac{1}{Z} + H_r \frac{1}{Z} \right) - a_2 G_r \cos\gamma + \frac{\partial P}{\partial z} \right] \cdot \left[8H_r + M^2 + \frac{1}{Z} + H_r \frac{1}{Z} \right] - \frac{\pi}{3Z} a_1 H_r - \frac{\pi}{6} Q a_2 G_r \cos\gamma \right\} h^6. \tag{3.4.2}$$

The values obtained for a_1 and a_2 are substituted into (3.4.2) to have expressions for the volumetric flow rate. The expression is not shown due to its length.

3.5 Wall Shear Stress

The wall shear stress, τ of the blood flow is defined as

$$\tau = \mu_0 \left[\frac{\partial w}{\partial r}\right]_{r=h}. \tag{3.5.1}$$

Substituting (3.3.5) into (3.5.1) and differentiating with respect to r, we obtain

$$\begin{aligned}\tau = &\left[\frac{a_1}{(1+H_r)}\left(M^2+\frac{1}{Z}+\frac{H_r}{Z}\right)-\frac{a_2 G_r\cos\gamma}{(1+H_r)}+\frac{1}{(1+H_r)}\frac{\partial P}{\partial z}\right]h\\ &+\left\{\frac{1}{12(1+H_r)^2}\left[a_1\left(M^2+\frac{1}{Z}+H_r\frac{1}{Z}\right)-a_2G_r\cos\gamma+\frac{\partial P}{\partial z}\right]\cdot\left[8H_r+M^2+\frac{1}{Z}+H_r\frac{1}{Z}\right]\right.\\ &\left.-\frac{4a_1H_r}{Z}-Qa_2G_r\cos\gamma\right\}h^3.\end{aligned} \tag{3.5.2}$$

The values obtained for a_1 and a_2 are substituted into (3.5.2) to have expression for the wall shear stress. The expression is not shown due to its length.

The wall shear stress, τ_s at the maximum height of the stenosis located at

$$z' = \frac{z}{b} = \frac{a}{b} + \frac{1}{n^{\frac{n}{n-1}}},$$

(the stenosis throat) is computed by assuming a negligible value of ξ in (2.7.15), and putting $h = 1-\delta$ [25]. Hence, we have

$$\tau_s = [\tau]_{h=(1-\delta)}. \tag{3.5.3}$$

4. Results, Summary and Conclusion

4.1 Results and Summary

The numerical computational results are simulated in the figures below in order to have greater insight into the qualitative analysis of the results. Various values of parameters controlling the blood flow system such as the magnetic field parameter (M), hematocrit parameter (H_r), porosity parameter (Z), heat source parameter (Q), Grashof number (G_r), Brinkman number (B_r), the angle of inclination, γ of the artery and the height of the stenosis (δ) were simulated through graphs plotted using the Mathematica software.

The following values of various parameters obtained from [25] were used:

$\partial P/\partial z = 0.3$, $M = 1.5$, $Z = 0.3$, $H_r = 1$, $G_r = 2$, $\gamma = \pi/3$, $Q = 1.5$, $B_r = E_c P_r = 2$, $\xi = 0.002$, $a = 0.25$, $b = 1$, $d_0 = 1$, $n = 2$, $z = 0.5$, $\delta = 0.1$, and $h = 0.923$.

4.1.1 Effects of the Different Parameters on Blood Velocity Profile. Figures 4.1a - 4.1h show the effect of the applied magnetic field on the velocity profile of blood.

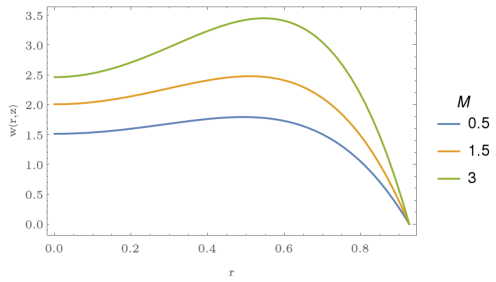

(a) Effects of Magnetic Field on Blood Velocity.

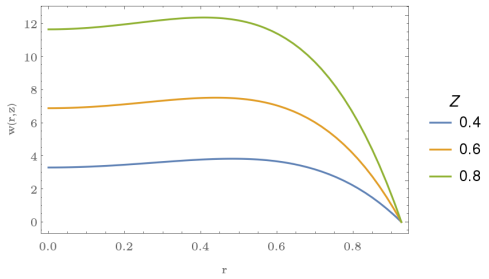

(b) Effects of Porosity on Blood Velocity.

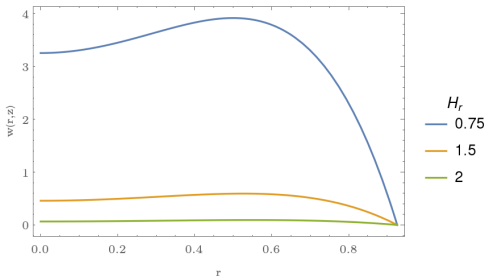

(c) Effects of Hematocrit on Blood Velocity.

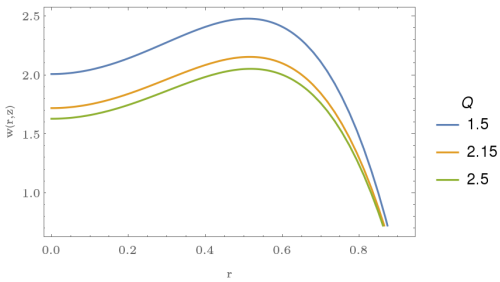

(d) Effects of the Heat Source on Blood Velocity.

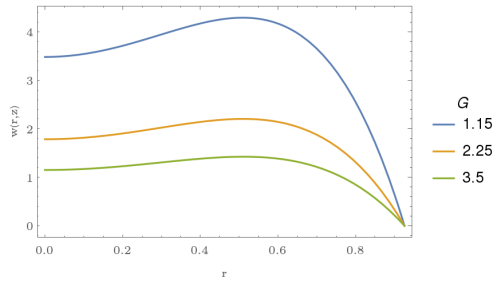

(e) Effects of Grashof Number on Blood Velocity.

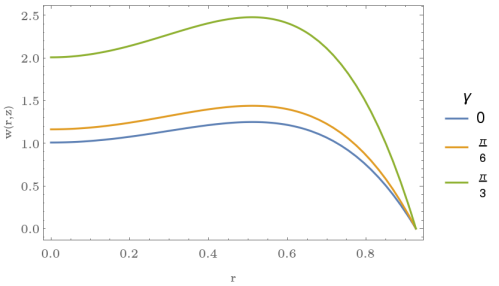

(f) Effects of the Inclination Angle on Blood Velocity.

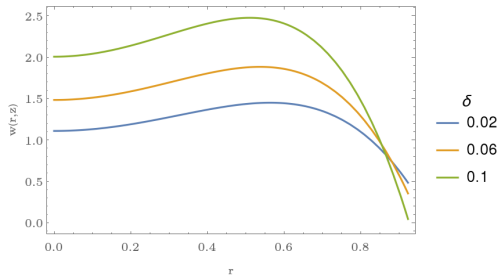

(g) Effects of the Stenosis Height on Blood Velocity.

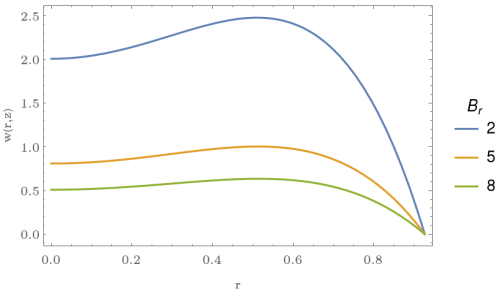

(h) Effects of Brinkman Number on Blood Velocity.

Figure 4.1: Variation of Velocity Profile of Blood Flow with Various Flow Parameters.

Figure 4.1a shows the behaviour of the axial velocity with the applied magnetic field. We see that the velocity increases as the magnetic field parameter increases. This occurs because the magnetic field is applied to a moving electrically conducting fluid and as these fields interact, the Lorentz force produced assists the motion of the blood.

Figure 4.1b depicts the behaviour of the velocity of blood with the porosity parameter. It can be seen that velocity of blood increases as the porosity parameter increases. This is because as more volume of empty spaces is added, fluid particles are able to move about in the artery more easily.

Figure 4.1c illustrates the behaviour of the velocity of blood with the hematocrit parameter. It shows that the velocity profile decreases as the hematocrit parameter increases. As the volumetric percentage of red blood blood cells increases, blood flow density increases which in turn slows down the flow of blood thereby, causing a decreased velocity of the blood flow.

Figure 4.1d describes how the velocity of blood varies with heat transfer. We see that the velocity of blood decreases with an increasing heat source.

Figure 4.1e represents the variation of the velocity of blood with the Grashof number. We see that an increase in the Grashof number leads to a decrease in the velocity of the blood flow.

Figure 4.1f shows the behaviour of the velocity of blood with the artery inclination angle. As the inclination angle of the artery increases from 0 to $\pi/3$, the velocity of blood flow increases.

Figure 4.1g indicates the behaviour of the velocity profile of blood as the stenotic height varies. It shows that the velocity of blood flow increases as the height of stenosis increases.

Figure 4.1h displays the behaviour of the velocity of blood with the Brinkman number. It is clear that, as the Brinkman number increases, the velocity of blood flow decreases.

4.1.2 Effects of the Different Parameters on Blood Temperature Profile. Figures 4.2a - 4.2h show the effect of the applied magnetic field on the velocity profile of blood.

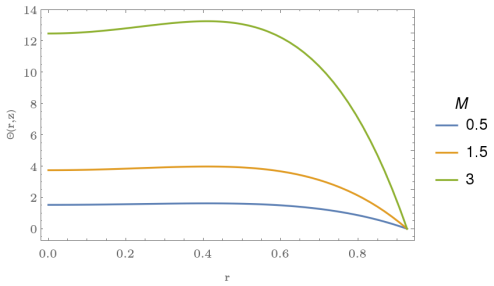

(a) Effects of Magnetic Field on Blood Temperature.

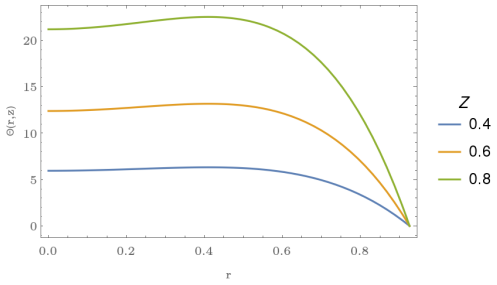

(b) Effects of Porosity on Blood Temperature.

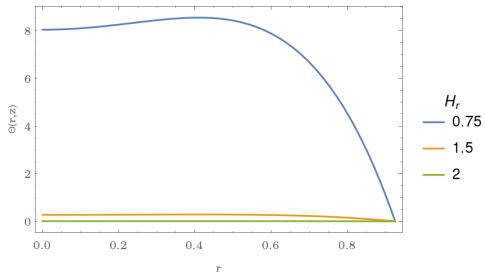

(c) Effects of Hematocrit on Blood Temperature.

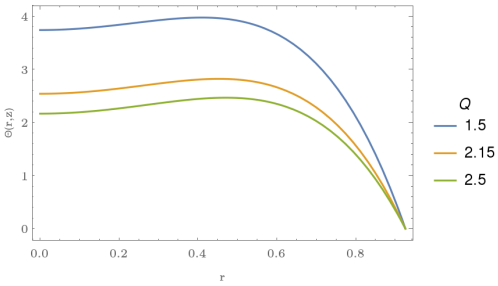

(d) Effects of the Heat Source on Blood Temperature.

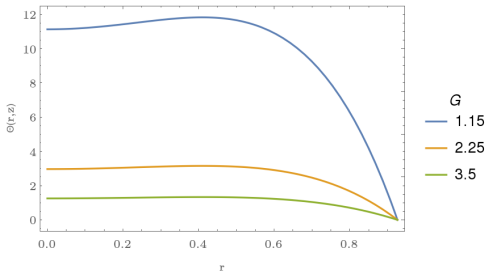

(e) Effects of Grashof Number on Blood Temperature.

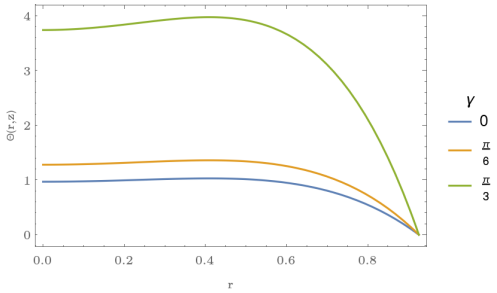

(f) Effects of the Inclination Angle on Blood Temperature.

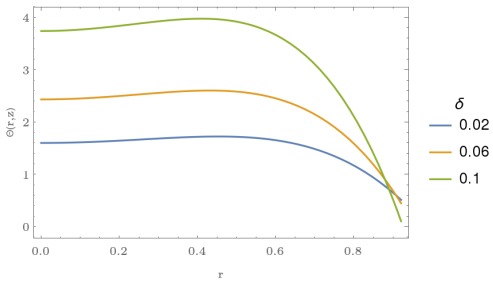

(g) Effects of the Stenosis Height on Blood Temperature.

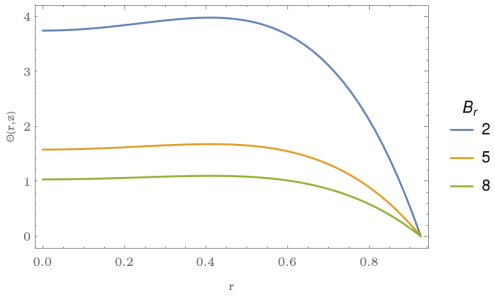

(h) Effects of Brinkman Number on Blood Temperature.

Figure 4.2: Variation of Temperature with Various Parameters.

Figure 4.2a represents how blood temperature varies with the applied magnetic field. It can be seen that the temperature profile increases as the magnetic field parameter increases.

Figure 4.2b shows the effect of porosity parameter on blood temperature. We see that the temperature profile increases as the porosity parameter increases. Blood is a viscous liquid, and with an increasing velocity, its viscosity decreases, hence, an increase in temperature.

Figure 4.2c represents the variation of the temperature of blood with the volume of red blood cells in the blood. It is clear that the temperature of blood decreases as the hematocrit increases. This is because of the viscous nature of blood. As the amount of red blood cells increases, interaction with the wall of the artery increases thereby, increasing the blood temperature.

Figure 4.2d indicates the effects of heat transfer within the blood on its temperature. We see that the temperature profile of blood decreases as the heat source parameter increases.

Figure 4.2e shows the effect of Grashof number on blood temperature. It is clear from the figure that the temperature of blood also decreases as the Grashof number increases.

Figure 4.2f shows how blood temperature varies as the inclination angle of the artery varies. It shows that the temperature of blood increases as the inclination angle increases.

Figure 4.2g indicates the behaviour of the temperature of blood with the height of the stenosis. The temperature of blood increases as the height of stenosis increases.

Figure 4.2h represents the behaviour of blood temperature with Brinkman number. It shows that the temperature of blood decreases as the Brinkman number increases.

4.1.3 Variation of Volumetric Flow Rate with the Tapering Parameter. Figures 4.3a - 4.3e show the effect of the applied magnetic field on the velocity profile of blood.

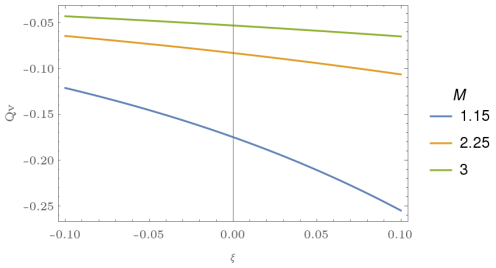

(a) Effects of Magnetic Field on Volumetric Flow Rate.

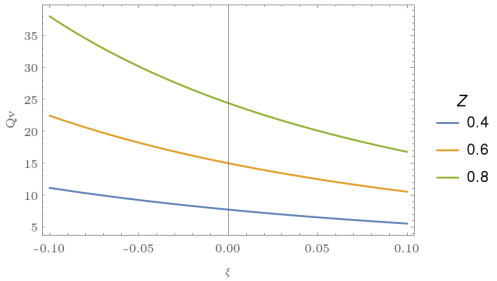

(b) Effects of Porosity on Volumetric Flow Rate.

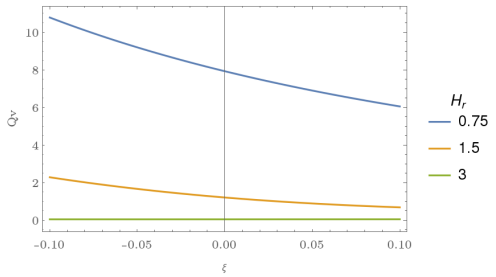

(c) Effects of Hematocrit on Volumetric Flow Rate.

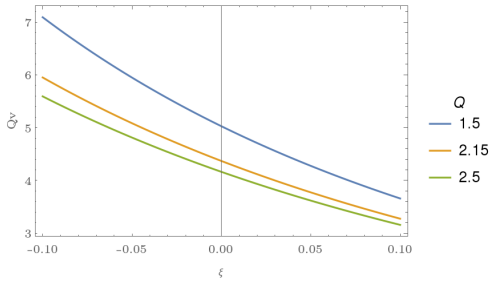

(d) Effects of the Heat Source on Volumetric Flow Rate.

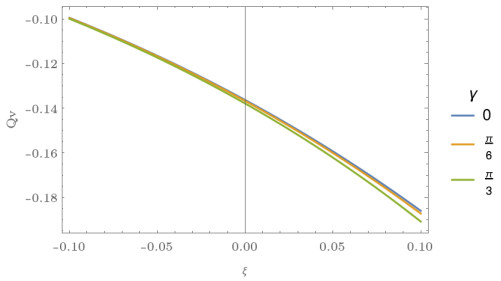

(e) Effects of the Inclination Angle on Volumetric Flow Rate.

Figure 4.3: Variation of Volumetric Flow Rate with Various Parameters.

Figure 4.3a shows the behaviour of the volumetric flow rate, Q_v in the diverging, converging and non-tapered regions of the artery with the external magnetic field. It can be seen that as the magnetic field increases, the volumetric flow rate increases in the diverging, converging and non-tapered regions.

Figure 4.3b shows the behaviour of the volumetric flow rate in the diverging, converging and non-tapered regions of the artery with the porosity parameter. We see that the volumetric flow rate increases as the porosity parameter increases.

Figure 4.3c represents the variation of the volumetric flow rate in the diverging, converging and non-tapered regions of the artery with the hematocrit parameter. It shows that the rate of blood flow decreases with an increasing volume of red blood cells.

Figure 4.3d indicates the behaviour of the volumetric flow rate in the diverging, converging and non-tapered regions of the artery with the rate of heat transfer. The rate of blood flow decreases with an

increasing heat source parameter.

Figure 4.3e shows the variation of the volumetric flow rate in the diverging, converging and non-tapered regions of the artery with the inclination angle of the artery. It shows that the volumetric flow rate decreases as the inclination angle increases from 0 to $\pi/3$.

4.1.4 Variation of Wall Shear Stress (τ_s) with the Height of Stenosis (δ). Figures 4.4a, 4.4b and 4.4c respectively indicate the variation of the wall shear stress at stenosis throat for different values of the magnetic field parameter (M), hematocrit parameter (H_r) and the porosity parameter (Z).

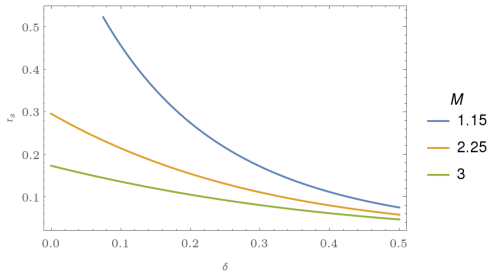

(a) Effects of Wall Shear Stress at Stenosis Throat with the Magnetic Field.

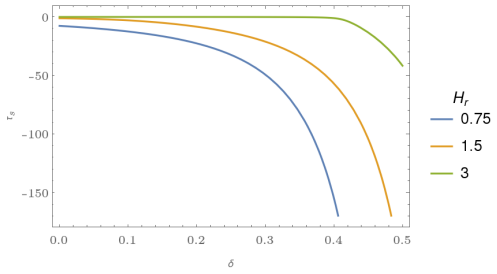

(b) Effects of Wall Shear Stress at Stenosis Throat with the Hematocrit Parameter.

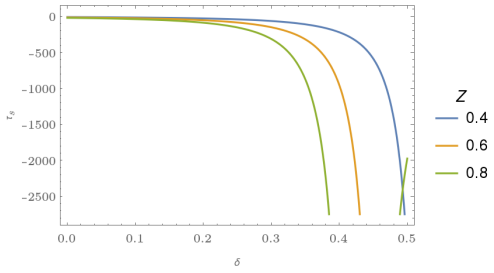

(c) Effects of Wall Shear Stress at Stenosis Throat with the Porosity Parameter.

Figure 4.4: Variation of Wall Shear Stress at Stenosis Throat.

Figure 4.4a shows that the wall shear stress decreases as the magnetic field parameter increases. We have seen that the magnetic field speeds up the blood flow and this allows the blood to flow with a reduced interaction with the walls of the artery, hence producing a minimal shear.

Figure 4.4b indicates the behaviour of wall shear stress as the hematocrit parameter varies. It shows that the wall shear stress increases as the hematocrit parameter increases in value.

Figure 4.4c displays how the wall shear stress varies as the porosity parameter varies. It shows that the wall shear stress decreases as the porosity parameter increases in value.

4.2 Conclusion

The electrically conducting blood in motion and the effects of an external magnetic field and heat transfer on the blood flow in an inclined tapered stenosed porous artery have been studied through this

project. The mathematical formulation for the momentum and energy equations was obtained for the blood flow considered to be Newtonian fluid. The resulting equations of motion were solved numerically using the Differential Transform Method (DTM). Various fluid parameters were used to study the effect of heat transfer and magnetic field on the velocity, temperature, volumetric flow rate and the wall shear stress of the blood. The following are the findings obtained:

1. An increase in the magnetic field parameter, M increases the velocity and temperature profiles of the blood flow due to the presence of the Lorentz force which assists the motion of the blood. The curves representing the volumetric flow rate show that the volumetric flow rate increases as the magnetic field parameter increases and is greater in the converging region as compared to the diverging region. It is however observed that the wall shear stress decreases at the stenosis throat as the magnetic field parameter increases.

2. An increase in the voids present in the porous medium increases the velocity and temperature profiles of the blood. With an increasing porosity parameter, the volumetric flow rate decreases greatly in the converging region of the artery as compared to the diverging and non-tapered regions. The wall shear stress decreases at the stenosis throat with an increasing porosity parameter.

3. Under the influence of heat transfer and magnetic field, there is a greater variation in the volumetric flow rate of an inclined artery in the converging region than in the diverging region.

4. More red blood cells in the blood means lesser velocity and temperature of the blood as the hematocrit parameter, H_r varies inversely as the velocity and temperature profiles. An increase in the hematocrit parameter increases the wall shear stress. The volumetric flow rate shows a reverse behaviour when the hematocrit parameter is increased and this behaviour is greater in the converging region than in the diverging region of the tapered artery.

5. By increasing the heat source parameter, we observed that the curves representing both the velocity and temperature profiles deviate rapidly from the origin. The volumetric flow rate varies inversely with the heat source parameter for converging, diverging and non-tapered regions of the artery.

6. It has been observed that, with heat transfer and applied magnetic field, the velocity and temperature profiles of blood in an inclined artery decrease as the Grashof number, G_r increases.

7. The Velocity and temperature profiles increase as the angle of inclination, γ of the artery increases. With the increase of inclination angle of the artery, it was observed that the volumetric flow rate will increase and will be more in the converging region than in the non-tapered and diverging regions of the artery.

8. With the increase in the height of stenosis, we observed that the velocity and temperature profiles increase, as the curves representing them shift away from the origin.

9. The curves describing the velocity and temperature profiles show the remarkable variation with Brinkman number. It was observed that, the higher the value of the Brinkman number, the higher the temperature rise of the blood. The velocity of blood flow was also observed to increase with an increasing value of Brinkman number.

Acknowledgements

I thank the Almighty God for His grace and protection over my life, making me successfully complete this programme without any form of sickness or casualty throughout.

I appreciate my project supervisor, Dr. Abubakar Usman Jos for keenly supervising my final project and for believing in my ability.

Thanks to the leadership of African Institute for Mathematical Sciences for giving me the rare opportunity of being part of the family. I am grateful to the lecturers, all the tutors and staff of AIMS, Cameroon for their contribution to the success of the programme.

I thank my parents for the solid support they have given to me up to this level.

Finally, I appreciate all my friends and colleagues in class for being wonderful and great collaborators in the various group works.

References

[1] Abdullah, I., Amin, N., and Hayat, T. (2011). Magnetohydrodynamic effects on blood flow through an irregular stenosis. *International Journal for Numerical Methods in Fluids*, 67(11):1624–1636.

[2] Akbarzadeh, P. (2016). Pulsatile magneto-hydrodynamic blood flows through porous blood vessels using a third grade non-newtonian fluids model. *Computer methods and programs in biomedicine*, 126:3–19.

[3] Bose, S. and Banerjee, M. (2015). Magnetic particle capture for biomagnetic fluid flow in stenosed aortic bifurcation considering particle–fluid coupling. *Journal of Magnetism and Magnetic Materials*, 385:32–46.

[4] Chakraborty, U. S., Biswas, D., and Paul, M. (2011). Suspension model blood flow through an inclined tube with an axially non-symmetrical stenosis. *Korea-Australia Rheology Journal*, 23(1):25.

[5] Department of Mechanical Engineering (Fall 2006). Marine hydrodynamics. [Online; accessed 15-April-2018. License: Creative Commons BY-NC-SA].

[6] El Jery, A., Hidouri, N., Magherbi, M., and Brahim, A. B. (2010). Effect of an external oriented magnetic field on entropy generation in natural convection. *Entropy*, 12(6):1391–1417.

[7] El-Shahed, M. (2003). Pulsatile flow of blood through a stenosed porous medium under periodic body acceleration. *Applied Mathematics and Computation*, 138(2-3):479–488.

[8] Fielding, S. (Autumn Semester 2005 (accessed April 10, 2018)). *Lecture on Laminar Boundary Layer Theory*.

[9] Kollin, A. (1936). Electromagnetic flowmeter: Principle of method and its application to blood flow measurement. *Proc. Soc. Exp. Biol. Med*, 35:53.

[10] Korchevskii, E. and Marochnik, L. (1965). Magnetohydrodynamic version of movement of blood. *Biophysics*, 10(2):411–414.

[11] Massey, B. S. and Ward-Smith, J. (1998). *Mechanics of fluids*, volume 1. Crc Press.

[12] Massoudi, M. and Christie, I. (1995). Effects of variable viscosity and viscous dissipation on the flow of a third grade fluid in a pipe. *International Journal of Non-Linear Mechanics*, 30(5):687–699.

[13] Mekheimer, K. S. and El Kot, M. (2008). The micropolar fluid model for blood flow through a tapered artery with a stenosis. *Acta Mechanica Sinica*, 24(6):637–644.

[14] Nadeem, S. and Akbar, N. S. (2009). Effects of heat transfer on the peristaltic transport of mhd newtonian fluid with variable viscosity: application of adomian decomposition method. *Communications in Nonlinear Science and Numerical Simulation*, 14(11):3844–3855.

[15] Nadeem, S., Akbar, N. S., Hayat, T., and Hendi, A. A. (2012). Influence of heat and mass transfer on newtonian biomagnetic fluid of blood flow through a tapered porous arteries with a stenosis. *Transport in porous media*, 91(1):81–100.

[16] Pantokratoras, A. (2006). The falkner–skan flow with constant wall temperature and variable viscosity. *International Journal of Thermal Sciences*, 45(4):378–389.

[17] Pedley, T. J. and Luo, X. (1995). *Fluid mechanics of large blood vessels*. Shaanxi People's Press.

[18] Petrofsky, J. S., Bains, G., Raju, C., Lohman, E., Berk, L., Prowse, M., Gunda, S., Madani, P., and Batt, J. (2009). The effect of the moisture content of a local heat source on the blood flow response of the skin. *Archives of dermatological research*, 301(8):581–585.

[19] Potter, M. (2009). *Fluid Mechanics DeMYSTiFied*. Demystified. McGraw-Hill Education.

[20] Prakash, O., Singh, S., Kumar, D., and Dwivedi, Y. (2011). A study of effects of heat source on mhd blood flow through bifurcated arteries. *AIP Advances*, 1(4):042128.

[21] Salih, A. (2011). Conservation equations of fluid dynamics.

[22] Shit, G. and Majee, S. (2015). Pulsatile flow of blood and heat transfer with variable viscosity under magnetic and vibration environment. *Journal of Magnetism and Magnetic Materials*, 388:106–115.

[23] Srivastava, N. (2014). Analysis of flow characteristics of the blood flowing through an inclined tapered porous artery with mild stenosis under the influence of an inclined magnetic field. *Journal of Biophysics*, 2014.

[24] Thongmoon, M. and Pusjuso, S. (2010). The numerical solutions of differential transform method and the laplace transform method for a system of differential equations. *Nonlinear Analysis: Hybrid Systems*, 4(3):425–431.

[25] Tripathi, B. and Sharma, B. K. (2016). Mhd blood flow and heat transfer through an inclined porous stenosed artery with variable viscosity. *arXiv preprint arXiv:1610.03470*.

[26] Young, D. (1968). Effect of a time-dependent stenosis on flow through a tube. *Journal of Engineering for Industry*, 90(2):248–254.

[27] Zhou, J. (1986). Differential transformation and its applications for electrical circuits.